Synthesis, Characterization, and Bioactivity Assessment of Rh(III) and VO(IV) Complexes with Isatin Derivative *N1*,*N2*-bis(2-oxoindolin-3-ylidene)ethanebis(thioamide)

Yusra Jalil Ahmed[1*], Shurooq Abdulfattah Hasan[1], Waeel Mohammed Hamud[1], and Nawal Hamdan Mahmoud[2]

[1]*Department of Chemistry, College of Science, Mustansiriyah University, Baghdad 10052, Iraq*

[2]*Department of Physics, College of Science, Mustansiriyah University, Baghdad 10052, Iraq*

* ***Corresponding author:***

email: yusrajalel@uomustansiriyah.edu.iq

Received: December 17, 2023
Accepted: March 14, 2024

DOI: 10.22146/ijc.91731

Abstract: *The new two-component complexes of Rh(III) as well as VO(IV), with the base of Schiff ligand associated with the isatin derivative* N1,N2-*bis(2-oxoindolin-3-ylidene)ethanebis(thioamide) (L) were prepared by one-step method reaction between isatin compound and dithiooxamide by condensation in presence of glacial acetic acid and investigated through applying the FTIR, UV-vis devices, evaluation of carbon, hydrogen, nitrogen and halogens elements using elemental analysis, flame atomic absorption, magnetic susceptibility, molar conductivity, GC-MS, LC-MS, XRD,* ^{1}H *and* ^{13}C*-NMR. Depending on the results obtained from the measurement techniques, the structure of Rh(III) complex was octahedral geometry, while VO(IV) complex was square pyramidal geometry. The antibacterial property for the prepared Schiff-based ligand L and metallic complexes 1 and 2 in this research was examined towards two different kinds about pathological microbes growth of* Escherichia coli *and* Staphylococcus aureus*, respectively, in comparison with conventional antibiotic cephalexin.*

Keywords: *azomethine ligand; thioamide derivative; rhodium(III) complex; oxovanadium(IV) complex; X-ray diffraction*

■ INTRODUCTION

The Schiff bases are important compounds for several applications in various fields, such as biological and analytical chemistry. The rules of its reactions provide many intermediate compounds important in all enzymatic reactions that interfere with an enzyme with an amino group or carbonyl substance [1]. Bases that contain isatin have a high affinity for chelating with transition metal ions and producing an extensive spectrum of biological effects, which involve as a painkiller and therapeutic for inflammation disease [2], anticonvulsant and antidepressant [3], antifungal [4], anticancer [5], antioxidant [6], antiviral [7-8], antitumor, anti-leukemic [9], and antiglycation activity [10]. Also, complexes of the transition metal ions with these ligands, as example Co^{2+}, Ce^{2+}, Pt^{2+}, UO_2^{2+}, Cu^{2+}, Mn^{2+}, Fe^{2+}, Fe^{3+}, Ni^{2+}, Cd^{2+}, and Rh^{3+}, which own different properties like biological, clinical, pharmacological as well as analytical features [5-8,11-14].

Isatin also named indole-2,3-dione itself; besides, the derivatives and complexes have given an extensive tabulate of biological activities against bacteria [1,14], fungi [4], cancer [5,9,11,15], viruses [8], as well as enzyme inhibitors [6]. Schiff bases that were prepared with isatin derivatives, which were substituted with various types of amines, has been recently diagnosed. The modern microwave method was used to obtain a solvent-free and antifungal product from their symmetries [1-2,5,7-9]. Different substituted groups in Schiff base compounds lead to the synthesis of different heterocyclic compounds. As a drug with severe side effects, researchers have increased interest in designing and developing alternative medicines containing derivatives for treating and resisting diseases with few or no side effects, which is the main reason for its high bio-

efficacy [16-17]. It seems the thioamide derivatives have not yet been a topic of numerous studies.

Dithiooxamide forms one of its derivatives, despite the fact that they appear in nature in bacteria and plants. This is because they are hard to separate and purify by employing standard methods in the lab. They require suitable solvent and temperature conditions; and almost all of their compounds are related to proteins, which makes them crucial for the assembly of enzymes like coenzyme. Their great efficacy is further enhanced by the abundance of both nitrogen and sulfur atoms in their composition, which offers them an advantage over amide derivative products in enzymatic reactions and makes them valuable intermediates in the manufacture of numerous pharmaceutical ingredients. Because of the important properties of dithiooxamide Schiff bases, like their semi-conductive, magnetic, spectroscopic, and thermal characteristics, these bases take an important place in different fields as well as their complexes. Also, Mannich base derivatives contain isatin and dithiooxamide, and their metal complexes have been investigated biologically [18].

Vanadium, as a rare metal, is important for organisms, though the lack of it in the human body has not been characterized till now [19]. The benefit of coordinated chemistry for vanadium VO(IV) in the medical area is the capability of vanadium-arisen to elevate the activity for insulin-mimetic at the condition of pathophysiology for diabetes mellitus in patients and as anticancer, antibacterial, and antifungal [20-21]. Rh(III) complexes with ligand like isatin and their Schiff base derivatives had significant field applications in drug synthesis to work on serious diseases, such as cancer, and these derivatives are more potent than other oxidation states Rh(II) and Rh(I) [22]. The mononuclear Rh(III) as organometallic drugs were used for wide purposes to inhibit various enzymes or cancers from 2013 till now [23-24]. Besides these properties, the octahedral Rh metal combination facilitated the immediate chemical substance-catalyzed alkylation for isatin molecules [25-26].

The target of our current work is studying the prepared ligand synthesized by condensing isatin with dithiooxamide. Two metal complexes for this ligand were prepared, and the prepared complexes were identified using various spectral and analytical devices. To reach the proposed chemical compositions, the biological effectiveness of these complexes against two bacteria was examined.

■ EXPERIMENTAL SECTION

Materials

Chemical materials were provided for the highest purity and were used as they were received. All were provided by Fluka, Aldrich, BDH, and Merck companies without any additional purification. We used isatin, dithiooxamide, vanadium(IV) oxide sulfate hydrate (97% purity, Sigma-Aldrich, USA), rhodium(III) chloride hydrate, *N*,*N*-dimethyl formamide (DMF), and chloroform (99.98% purity, BDH, UK), dimethyl sulfoxide (99.5% purity, Sigma-Aldrich, USA), silver nitrate (99.0% purity, Sigma-Aldrich, USA), dichloromethane (99.5%, Merck, Germany), glacial acetic acid (100% purity, Merck, Germany), and ethanol absolute (99% purity, Merck, Germany).

Instrumentation

The prepared ligand, along with each of the complexes' melt temperatures, have been identified as well as generated *via* the SMP30 apparatus, and the elemental analysis was found by utilizing C.H.N.S Italy Eurovector instruments and software. The percentage of metal transitions in the two prepared complexes was estimated by flame atomic absorption (FIA) using the Shimadzu-670 AA spectrophotometer. As well as the data of infrared spectra were assigned by using the device FT-IR-8300 Shimadzu in the range 200–4000 cm^{-1}, and the sample disc was prepared in CsI for the two complexes only, and Bruker Alpha II estimated the ligand in the range 400–4000 cm^{-1}. The determination of susceptibility measurements of samples in their solid state was achieved using Faraday's method, which used the Balance Magnetic Susceptibility Modal MSB-MKI apparatus. The molar conductivity for the two complexes was measured by using the electrolytic conductivity device model WTW conductivity photometer series 82362 Weilheim. The

platinum electrode of the device was type EDC 304, the cell constant was 1 cm, and the concentration was 1×10^{-3} M. The used solvent is DMSO at 25 °C. Electronic spectra were measured using the UV-visible spectrophotometer Varian apparatus at 25 °C with 1×10^{-3} M concentrations for all prepared ligands and complexes in DMSO. GC-MS was recorded by using GC-MS Ultra QP2010 Shimadzu for the ligand. As for the liquid chromatography/mass spectrometry detection for the Rh(III) and VO(IV) complexes with synthetic ligand L, it was performed using an AB Sciex 3200 QTRAP LC-MS/MS system at Basra University, College of Science. NMR spectra were acquired in DMSO-d_6 on a Varian 400 MHz spectrometer at 400 to feed ^{1}H and 100 MHz to earn ^{13}C, applying a tetramethylsilane known as TMS, as the standard. Rh(III) and VO(IV) complexes were diagnosed using X-ray diffraction (XRD) spectroscopy on the Phillips Analytical X'Pert device.

Procedure

The preparation of the ligand

Isatin (0.294 g, 2 mmol) was dissolved in 20 mL of hot ethanol, then dithiooxamide (0.120 g, 1 mmol) was added, and followed by a few drops of glacial acetic acid. The mix solution was heated up for over 4 h before being brought down to the normal temperature of 25 °C. The precipitate was filtered and recrystallized with pure ethanol. The yield of Schiff base ligand L was determined in Scheme 1. Physical and chemical characteristics for synthesized ligand were recorded and listed in Table 1.

The preparation of complexes (1-2)

Metal salts of $RhCl_3 \cdot 3H_2O$ (0.263 g, 1 mmol) and $VOSO_4 \cdot 3H_2O$ (0.217 g, 1 mmol) were dispersed into 10 mL hot ethanol and poured into 0.378 g (1 mmol) amount for ligand that was dissolved in 10 mL ethanol with stirring. These mixtures were heated for 1 h under reflux. As refluxing time finished, precipitates were produced, and the crystals of the complexes grew in the mother solution in a cold environment for 20 d, which led to the formation of pure crystals. Then, these precipitates were washed more than once in a watery ethanol mixture and dried under vacuum. Their molar ratio was 1:1 metal:ligand, as proved by Job's method of continuous variation [11]. The physical properties of prepared complexes 1 and 2 are listed in Table 1.

Bio-microorganism action study

The synthetically produced substances were examined for anti-microbial properties towards the bacteria *S. aureus* (ATCC 25923) and *E. coli* (ATCC 25922), employing the agar-based plate diffusion approach [18]. The already-prepared agar and the petri dishes were sterilized by autoclave for a period of 15 min, around 121 °C. Those agar plates had been carefully infused with a broth that contained cultures from the evaluated microbial organisms. To completely fill all the solid medium, 100 mL of each of the formed substances were inserted into properly spaced 6 mm-diameter holes. Our manufactured molecules were dispersed within the dimethyl sulfoxide solvent at 500 and 1000 µg/mL. The agar plates were left to incubate at a temperature of 37 °C for 24 h. Then, the area that inhibited growth was calculated using mm diameters for every compound utilized during the current investigation.

■ RESULTS AND DISCUSSION

Elemental Analysis

The physical and analytical features for each synthesized ligand and complexes 1 and 2 were listed in Table 1. The information gained from recording the elemental analysis measurements is complementary with

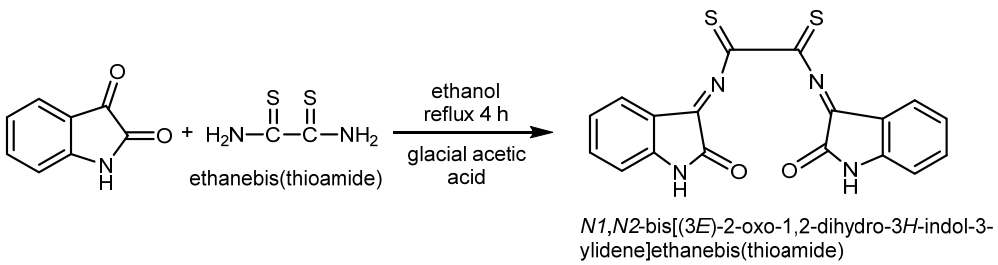

Scheme 1. The preparation of the ligand L

Table 1. The chemical and physical characteristics of the ligand L, complexes 1, and 2

Name	Color	Melting point or Decomposition temperature (°C)	Yield% weight (g) Mol. weight (g/mol)	Elemental microanalysis % Found (Calc.)						Formula
				C%	H%	N%	S%	O%	M%	
L	Red	181–182	66.13% 0.5 378	57.20 (57.14)	2.34 (2.64)	14.44 (14.81)	16.33 (16.93)	8.28 (8.46)	--	$C_{18}H_{10}N_4S_2O_2$
1	Brown	240*	51.06% 0.3 587.5	36.50 (36.79)	1.63 (1.72)	9.26 (9.53)	10.10 (10.91)	--	17.77 (17.53)	$[Rh(C_{18}H_{10}N_4S_2O_2)Cl_2]Cl$
2	Brown	270*	77.63% 0.42 541	39.57 (39.93)	1.74 (1.86)	10.29 (10.35)	17.78 (17.77)	--	9.58 (9.42)	$[VO(C_{18}H_{10}N_4S_2O_2)]SO_4$

Note: * = decompose

the experimental value. The molecular formula was suggested according to the spectral gained data which match with the magnetic moment. The colored crystalline solid precipitates were dissolved in CH_2Cl_2, $CHCl_3$, DMF, and DMSO. These compounds settled firm throughout heating and were unaffected by the O_2 atmosphere or water.

FTIR Spectrum Study

FTIR properties associated with the constructed ligand L

The FTIR spectrum of ligand L is displayed in Fig. 1(a) and Table 2. The prepared ligand gave appearing a band of –NH assigned at 3447 cm^{-1} [27-28], –C=O of the ketone group appeared at 1606 cm^{-1}, –C=N found at 1565 cm^{-1}, and this band of azomethine confirms the formation of the Schiff base [18-29], and –C=S showed absorption band in the region 1383 cm^{-1} [30]. The other two bands at the region 840 and 742 cm^{-1} refer to di-substituted for the aromatic ring [17-18].

FTIR spectrum of complex 1

The FTIR spectrum of complex 1 is presented in Fig. 1(b). Table 2 showed a band of –C=O, which had been displaced to a lower wavenumber to appear at 1633 cm^{-1}, and a band of –C=N appeared at 1595 cm^{-1}, which means that it becomes linked with the Rh(III) metal *via* the N atom from –C=N related to the isatin ring and the O from the ketone molecule [24]. New bands appeared from the spectrum, including the complex in regions 586, 414, and 304 cm^{-1} attributed to M–N, M–O, and M–Cl, following one another [22,30].

FTIR spectrum of complex 2

The FTIR spectrum of the prepared complex 2 was illustrated in Fig. 1(c). Table 2 identified strong bands located in the ligand attributed by the C=O and C=N groups, as well, at 1606 and 1565 cm^{-1} [11], were shifted to regions at 1644 and 1596 cm^{-1}. This means that –C=O and –C=N bonds are associated with vanadium(IV) oxide, with no M–Cl band availability. For this complex, a band appeared at 1087 cm^{-1}, which is assigned to $\nu(SO_4)$ [20,31-32], as well as showed a band of ν(V=O) at the region 989 cm^{-1} [31]. A new band appeared, indicating the existence of M–L bands where the FTIR region appears at 424 and 538 cm^{-1} assigned to M–O and M–N, consecutively [21].

Magnetic Moments

All values of magnetic moments μ_{eff} in Bohr magneton (B.M) unit were found at 25 °C for the prepared

Table 2. The vibrational rates in cm^{-1} area bands for the non-conjugate ligand and related complexes 1 and 2

Name	$\nu(SO_4)$	ν(V=O)	ν(C=S)	ν(C=O)	ν(C=N)	ν(M–N)	ν(M–O)	ν(M–Cl)
L	-	-	1383	1606	1565	-	-	-
1	-	-	1380	1633	1595	586	414	304
2	1087	989	1381	1644	1596	538	424	-

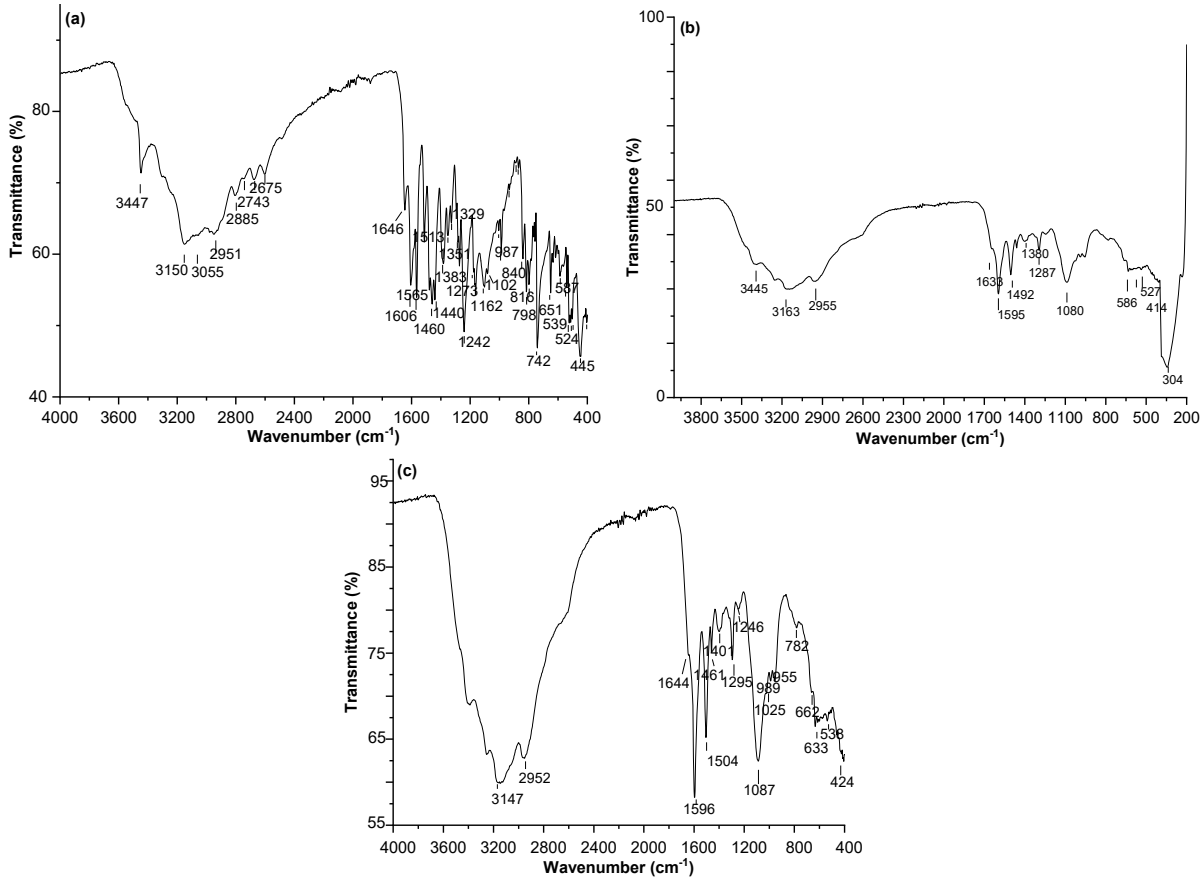

Fig 1. FTIR spectrum of (a) prepared ligand, (b) complex 1, and (c) 2

complexes (1-2) recorded in Table 3. These values for solid complex 1 were 2.3 B.M, which referred to two unpaired electrons with an octahedral shape [26]. These data agreed with the electronic spectra measurements. The value of the μ_{eff} for complex 2 was 1.68 B.M, which referred to two unpaired electrons [21-22], which means that this complex has a square pyramidal shape.

Electronic UV-Vis Spectroscopic Study

The electronic UV-vis spectrum of ligand L

The UV-vis data of L is presented in Fig. 2(a) and Table 3. The L's spectrum measurements exhibited an intense band at the location 207 nm (48309 cm^{-1}), which represents transitions $\pi \rightarrow \pi^*$, and two other bands appeared in the two regions 240 (41666 cm^{-1}) and 247 nm (40485 cm^{-1}), which referred to $n \rightarrow \pi^*$ transitions [9,17].

Electronic UV-vis spectrum of complex 1

The UV-vis spectrum of complex 1 is presented in Fig. 2(b) and Table 3. Complex 1 displayed three absorption bands in the regions 453 (22075 cm^{-1}), 889 (11248 cm^{-1}), and 978 nm (10224 cm^{-1}). These spectra referred to the three electronic transitions $^2T_2g \rightarrow {}^2A_2g$, $^2T_2g \rightarrow {}^4T_2g$, and $^2T_2g \rightarrow {}^4T_1g$, respectively, which means that the complex is octahedral shape [23,26,33-34].

Electronic UV-vis spectrum of complex 2

The UV-vis spectrum of complex 2 is presented in Fig. 2(c) and Table 3. Complex 2 has a band in the region 410 (24390 cm^{-1}), and three bands in 574 (17421 cm^{-1}), 584 (17123 cm^{-1}), and 890 nm (11235 cm^{-1}). These bands referred to electronic transitions of L→V (C.T) [11,14-15], $^2B_{2g} \rightarrow {}^2E_g$, $^2B_{2g} \rightarrow {}^2B_{1g}$, and $^2B_{2g} \rightarrow {}^2A_{1g}$ respectively, which means that this complex is square pyramidal in shape [21-22,35].

Molar Conductivity

The values of molar conductivity represented the complexes 1 and 2 outlined in Table 3 were gained by using 1×10^{-3} M concentration prepared with the typical

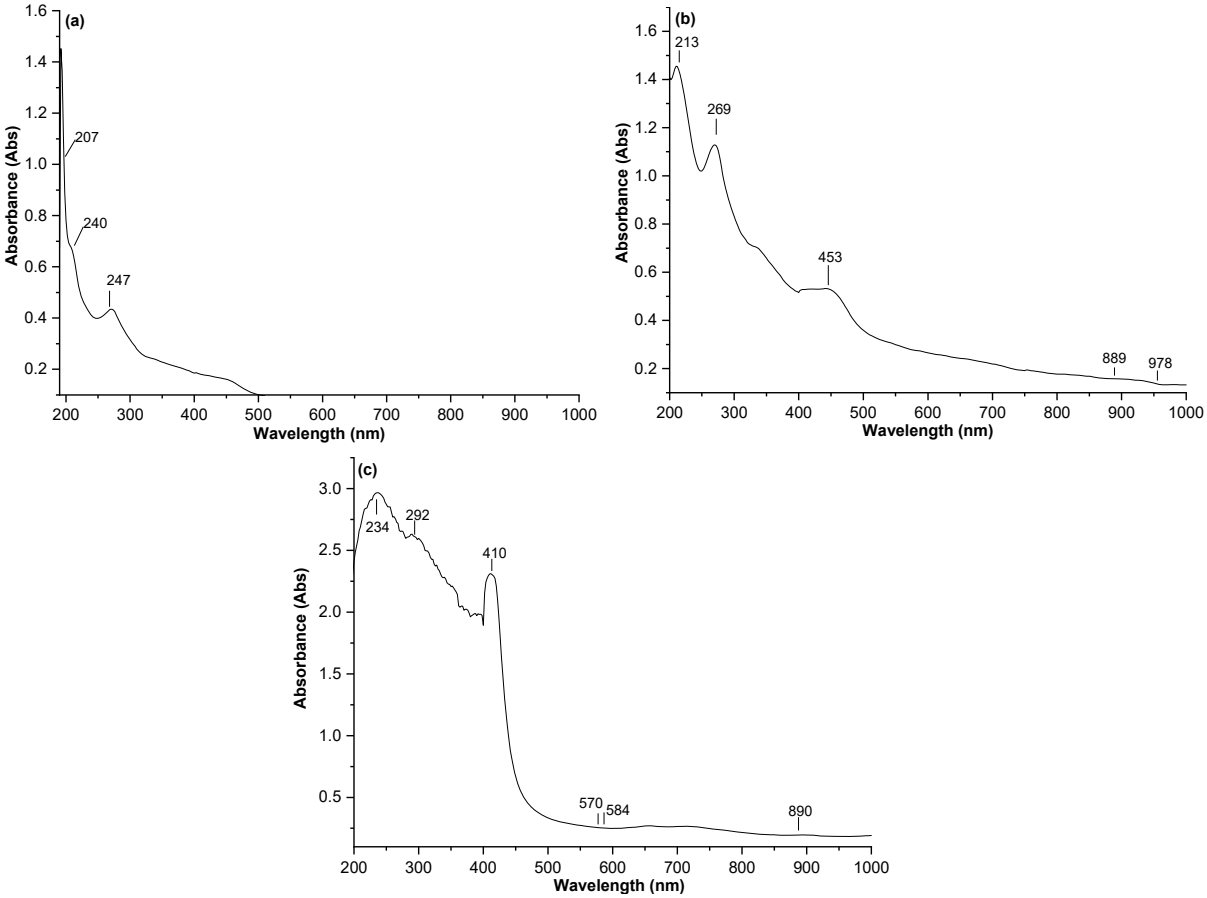

Fig 2. UV-vis spectrum of (a) free ligand (L), complex (b) 1, and (c) 2

Table 3. Electronic spectra, molar conductance, as well as magnetic moment of ligand and its prepared complexes 1 and 2

Name	Wavelength λ (nm), Wavenumber ν (cm^{-1})	Assignment	μ_{eff} (B.M)	Molar ratio M:L	Molar conductance (Ohm^{-1} cm^2 mol^{-1}) in DMSO	Geometry
L	207, 48309	π→π*	-	-	-	-
	240, 41666	n→π*				
	247, 40485	n→π*				
1	453, 22075	$^2T_2g \rightarrow {}^2A_2g$	2.3	1:1	32.2	Octahedral
	889, 11248	$^2T_2g \rightarrow {}^4T_2g$				
	978, 10224	$^2T_2g \rightarrow {}^4T_1g$				
2	410, 24390	(L) →V (C.T)	1.68	1:1	36.5	Square pyramidal
	574, 17421	$^2B_2g \rightarrow {}^2Eg$				
	584, 17123	$^2B_2g \rightarrow {}^2B_1g$				
	890, 11235	$^2B_2g \rightarrow {}^2A_1g$				

laboratory conditions at room temperature of 25 °C within the dimethyl sulfoxide, a common solvent. The results obtained for the prepared complexes are electrolytic of the type 1:1.

Mass, ^{1}H-NMR, and ^{13}C-NMR Spectra of All Prepared Compounds (L, 1, and 2)

The mass spectrum of L additionally its corresponding complexes one and two observed an ion

peak towards *m/z* of 378, 587, and 541 amu related to $[M]^+=[C_{18}H_{10}N_4S_2O_2]^+$, $[[Rh(C_{18}H_{10}N_4S_2O_2)Cl_2]Cl]^+$, and $[[VO(C_{18}H_{10}N_4S_2O_2)]SO_4]^+$, respectively. The percentages of relative intensity abundance of 51.0, 40.0, and 100.0%, respectively, in the sample showed that they matched their proposed structure and calculated molecular weight precisely 378, 587, and 541 g/mol, respectively. Fig. 3 refers to the mass spectrum of L.

The ligand L's ^{1}H-NMR measurements using the solvent $(CD_3)_2SO$ showed singlet signal shift δ at 9.64 ppm (s, 2H, 2NH), which could be attributed to –NH of two isatin rings. Signals shift appeared at range 6.78–7.99 ppm (m, 8H, 2Ar-H) as multiple signals of two phenyl rings in ligand L. The spectrum revealed peaks at 3.02–2.48 ppm that come from the signal of the solvent, which is DMSO-d_6.

Finding results of the ^{13}C-NMR in DMSO-d_6 spectrum of L shows characteristic signals that can be assigned as follows: at 189.40 ppm for C=S group, at 144.39 ppm for carbon of the first azomethine C=N group, at 135.55 ppm for carbon of the second azomethine C=N, at 135.35 ppm for the first C=O group, at 135.25 ppm for the second C=O group, at 132.82, 131.13, 130.98, 130.10, 129.42, 129.18, 128.96, 128.20, 127.45, 124.61, and 122.58 ppm signals meaning that they correlate to all of the carbon-based atoms that compose the aromatic system of two phenyl groups in the ligand, and 40.43–39.60 ppm for DMSO-d_6 solvent.

XRD of Prepared Complexes 1 and 2

In this study, the XRD measurement results for Rh(III) and VO(IV) complexes were matched with the standard parameters found in the database of the International Diffraction Information Center and the Cambridge Crystallography Center. They provide proof of the crystalline nature of the complexes, which shows us the geometric shape of the prepared complexes accurately. After examining the complex 1 diffractogram, the sharp peaks at 2θ angles as in Fig. 4, showed a hexagonal crystal structure, which matches the data card reference (JCPDS Card No. 05-0685) and affirms the P36mc space group, following the Trellis parameters a = b= 18.2000 Å, c = 5.4330 Å, and also α = β = 90.0° and γ = 120.0° [36].

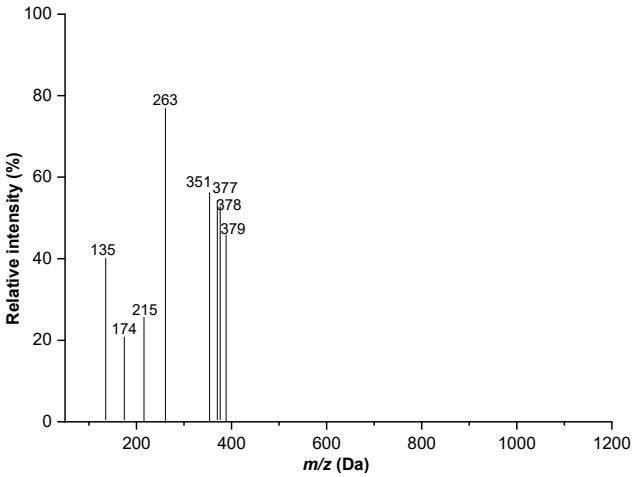

Fig 3. Mass spectrum of ligand (L)

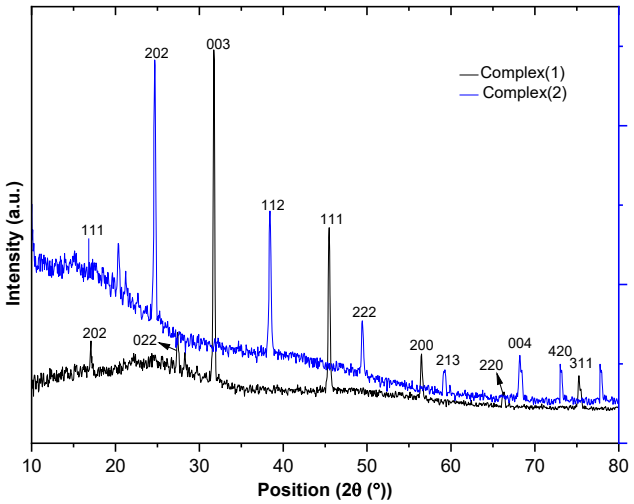

Fig 4. XRD pattern of complex (1) and complex (2) at 25 °C

The complex 2 XRD spectra convey strong, sharp peak levels at angles of 2θ = 16.83° and 44.90°, as in Fig. 4, confirming a monoclinic lattice crystal with potential geometry as a square pyramid, which matches the data of the Cambridge Crystallography Center (CCDC No. 987361), which goes back to the C2/m space group. Along with the subsequent trellis constants as a = 21.4154 Å, b = 4.8975 Å, and c = 9.2043 Å, then α = 90.0°, β = 108.0°, and γ = 90.0° [37]. Table 4 lists values for the crystal levels and the angle 2θ for complexes 1 and 2.

The Structure and Stereochemistry

The results obtained from elemental analysis and spectral data, which are consistent with magnetic moment,

Table 4. The angle 2θ and crystalline levels for the prepared complexes

No. complexes	2θ (°)	Crystal levels (hkI)
1	17.07	202
	27.39	022
	31.66	003
	45.49	111
	56.47	200
	66.24	220
	75.34	311
2	16.83	111
	28.35	202
	30.86	112
	44.90	222
	56.43	213
	65.82	004
	74.73	420

molar conductivity data, XRD measurement results, and other analysis tools for complexes 1 and 2, lead to suggesting the geometric configuration regarding the prepared compounds, which can be observed in Fig. 5(a), showing that the complex 1 has an octahedral shape, and in Fig. 5(b), showing that the complex 2 is square-pyramidal in shape. It had been found that the substance being studied, L is a tetradentate type with a neutral charge coordinated with two nitrogen atoms and two oxygen atoms with Rh(III), a trivalent element in nature, and two negative ion charges signifying chlorine within the coordination sphere and a chloride atom outside. In practice, chloride can be detected by a solution of silver nitrate [35], so we drop it upon a solution with a concentration of 1×10^{-1} M of Rh complex to confirm its existence; white precipitation indicates the presence of the chloride ion outside. The VO(IV) metal interacted with L *via* 2 N and 2 O atoms and equalized coordinated charges in the presence of SO_4^{2-} as a counter ion, and no chloride atom was observed based on the various measurements done for this complex. It has also been proven through the $AgNO_3$ solution test that it did not show any precipitation.

Biological Response Results

The newly synthesized compounds were evaluated as antibacterial agents *in vitro* against two bacteria strains, *S. aureus* (a Gram-positive bacteria) and *E. coli* (a Gram-negative bacteria). This research tested only two concentrations (500 and 1000 μg/mL) due to their effectiveness and importance [33]. The findings and data are documented in Table 5. The outcome values of the inhibitory zone show the bionature of L had weak action concerning both Gram-positive and Gram-negative bacteria in 500 μg/mL concentration, and also showed weak activity over Gram-negative bacteria in 1000 μg/mL concentration, while showing high activity upon Gram-positive bacteria in 1000 μg/mL concentration. Complex 1 showed weak activity in 500 μg/mL concentration and modesty responses with 1000 μg/mL concentration towards *E. coli* bacteria. It was observed that it showed moderate activity in 500 μg/mL concentration to high activity in 1000 μg/mL concentration towards *S. aureus* bacteria. Otherwise, the complex 2 showed moderate activity in 500 μg/mL concentration towards *S. aureus*

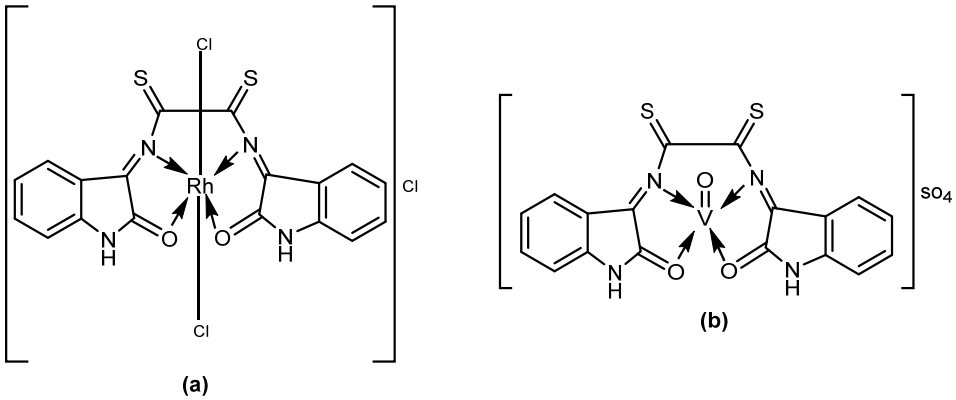

Fig 5. The suggested structure of complex (a) 1 and (b) 2

Table 5. Biological effects caused by the formed chemical compounds regarding 500 and 1000 µg/mL concentrations on the selected strains of bacteria reflected cephalexin as standard drug presented in inhibition zone (mm)

Name	*Escherichia coli*		*Staphylococcus aureus*	
	500 µg/mL	1000 µg/mL	500 µg/mL	1000 µg/mL
Control DMSO	0	0	0	0
Cephalexin	20	30	27	30
L	11	14	14	22
1	15	18	20	24
2	20	21	19	22

Note: The absence of activity is defined as a minimum of 10 mm, low activeness as 10–15 mm, moderate level of activity as 15–20 mm, and elevated activation as over 20 mm

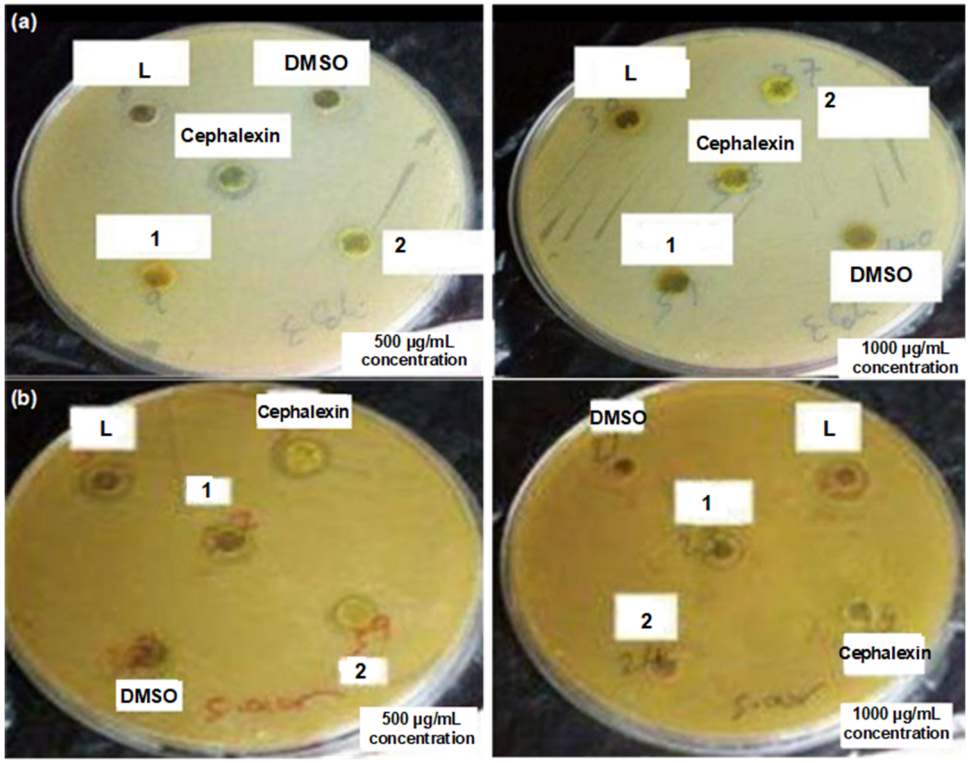

Fig 6. Effects of the synthetic chemicals and cephalexin on the chosen cultures of (a) *E. coli* and (b) *S.* aureus pathogens

and *E. coli* selected bacteria strains, whereas in 1000 µg/mL concentration, it showed high activity towards *E. coli* and *S. aureus* selected bacteria strains with inhibition zone ranged from 21–22 mm. These results show that the type of substituents in the ligand molecule and complexes with transitional elements play a vital role in enhancing the beneficial effects of such synthesized substances in comparison to cephalexin, the conventional medication that showed activity with inhibition zone ranged from 20–30 mm in 500 and 1000 µg/mL concentrations towards the same type of bacteria in this research. The inhibition zone images represented the activity of the synthesized compounds ligand L, complexes 1 and 2, and cephalexin drug can be seen in Fig. 6(a) and (b) for the *E. coli* and *S. aureus* selected bacteria strains, respectively.

■ CONCLUSION

In this study, complex 1 was octahedral geometry, and complex 2 was square pyramidal geometry. After

using several analytical tools to prove the exact structure and geometric shape of the prepared complexes and ligand, which had never been prepared before, even so far, the study successfully obtained the prepared compounds by the methods explained in this paper. Also, the investigation was conducted about the complexes' biological activities that ranged from weakly to moderately effective actions versus two different kinds of microbes in contrast to the ligand (L) prepared, and compared with the standard drug cephalexin could give the complexes prepared to be considered as new future applications as antibacterial agents.

■ ACKNOWLEDGMENTS

The researchers are grateful and thank Mustansiriyah University, Baghdad, Iraq (https://uomustansiriyah.edu.iq), for support and access to facilities and Ibn Sina Company Laboratories to help them complete this study.

■ CONFLICT OF INTEREST

The authors show they have not received any financial support from any person or institution to influence this paper.

■ AUTHOR CONTRIBUTIONS

The first author Yusra Jalil Ahmed designed the methods of research. The second and third researchers participated with Yusra Jalil Ahmed in the method of preparing the compounds, analysing them, and measuring them using various spectroscopic devices and XRD as well. Nawal Hamdan Mahmoud coordinated the research language and interpreted the measurements and results obtained for the compounds. All authors agreed to the final version of this manuscript.

■ REFERENCES

[1] Lahari, K., and Sundararajan, R., 2020, Design and synthesis of novel isatin derivatives as potent analgesic, anti-inflammatory and antimicrobial agents, *J. Chem. Sci.*, 132 (1), 94.

[2] Dantas, L.L.S.F.R., Fonseca, A.G., Pereira, J.R., Furtado, A.A., Gomes, P.A.T.M., Fernandes-Pedrosa, M.F., Leite, A.C.L., Rêgo, M.J.B.M., Pitta, M.G.R., and Lemos, T.M.A.M., 2020, Anti-inflammatory and antinociceptive effects of the isatin derivative (*Z*)-2-(5-chloro-2-oxoindolin-3ylidene)-*N*-phenyl-hydrazinecarbothioamide in mice, *Braz. J. Med. Biol. Res.*, 53 (10), e10204.

[3] Zhen, X., Peng, Z., Zhao, S., Han, Y., Jin, Q., and Guan, L., 2015, Synthesis, potential anticonvulsant and antidepressant effects of 2-(5-methyl-2,3-dioxoindolin-1-yl)acetamide derivatives, *Acta Pharm. Sin. B*, 5 (4), 343–349.

[4] Dar, O.A., Lone, S.A., Malik, M.A., Aqlan, F.M., Wani, M.Y., Hashmi, A.A., and Ahmad, A., 2019, Synthesis and synergistic studies of Isatin based mixed ligand complexes as potential antifungal therapeutic agents, *Heliyon*, 5 (7), e02055.

[5] Subin Kumar, K., Reena, V.N., and Aravindakshan, K.K., 2021, Synthesis, anticancer and larvicidal activities of a novel Schiff base ligand, 3-((2-((1-(4-hydroxyphenyl)ethylidene)amino)ethyl)imino)-*N*-(*p*-tolyl)butanamide and its Mn(II), Fe(III), Co(II), Ni(II) and Zn(II) complexes, *Results Chem.*, 3, 100166.

[6] Vairalaksmi, M., Princess, R., and Johnson Raja, S., 2019, The metal complexes of novel Schiff base containing isatin: Characterization, antimicrobial, antioxidant, and catalytic activity study, *Asian J. Pharm. Clin. Res.*, 12 (8), 206–210.

[7] Khan, T., Raza, S., and Lawrence, A.J., 2022, Medicinal utility of thiosemicarbazones with special reference to mixed ligand and mixed metal complexes: A review, *Russ. J. Coord. Chem.*, 48 (12), 877–895.

[8] Seema, S., Kumari, S., and Ranka, M., 2020, Mixed ligand complex of Ni(II) with Schiff base ligands derived from isatin and its bromo derivative: Synthesis, characterization and biological screening, *Int. J. Chem. Sci.*, 18 (2), 301.

[9] Arshad, N., Mir, M.I., Perveen, F., Javed, A., Javaid, M., Saeed, A., Channar, P.A., Farooqi, S.I., Alkahtani, S., and Anwar, J., 2022, Investigations on anticancer potentials by DNA binding and cytotoxicity studies for newly synthesized and characterized imidazolidine and thiazolidine-based isatin derivatives, *Molecules*, 27 (2), 354.

[10] Jamil, W., Solangi, S., Ali, M., Khan, K.M., Taha, M., and Khuhawar, M.Y., 2019, Syntheses, characterization, *in vitro* antiglycation and DPPH radical scavenging activities of isatin salicylhydrazidehydrazone and its Mn(II), Co(II), Ni(II), Cu(II), and Zn(II) metal complexes, *Arabian J. Chem.*, 12 (8), 2262–2269.

[11] Sohrabi, M., Saeedi, M., Larijani, B., and Mahdavi, M., 2021, Recent advances in biological activities of rhodium complexes: Their applications in drug discovery research, *Eur. J. Med. Chem.*, 216, 113308.

[12] Wu, Z., Zhang, Z., Ding, L., Xiang, M., and Luo, S., 2020, Development of a novel octahedron rhodium complex and its application to the alkynylation of isatin derivatives, *Tetrahedron Lett.*, 61 (48), 152577.

[13] Albayati, A., Sheet, S., and Haydari, A., 2023, Synthesis and characterization of New binuclear complexes of Fe(II), Co(II), Zn (II), and Cd(II) with Schiff base ligands derived from isatins and amines, spectroscopic study and evaluation of their biological activity, *Egypt. J. Chem.*, 66 (2), 411–424.

[14] Yan, X., Lv, Z., Wen, J., Zhao, S., and Xu, Z., 2018, Synthesis and *in vitro* evaluation of novel substituted isatin-propylene-1*H*-1,2,3-triazole-4-methylene-moxifloxacin hybrids for their anti-mycobacterial activities, *Eur. J. Med. Chem.*, 143, 899–904.

[15] Chowdhary, S., Shalini, S., Arora, A., and Kumar, V., 2022, A mini review on Isatin, an anticancer scaffold with potential activities against neglected tropical diseases (NTDs), *Pharmaceuticals*, 15 (5), 536.

[16] Haj Mohammad Ebrahim Tehrani, K., Hashemi, M., Hassan, M., Kobarfard, F., and Mohebbi, S., 2016, Synthesis and antibacterial activity of Schiff bases of 5-substituted isatins, *Chin. Chem. Lett.*, 27 (2), 221–225.

[17] Szklarzewicz, J., Jurowska, A., Matoga, D., Kruczała, K., Kazek, G., Mordyl, B., Sapa, J., and Papież, M., 2020, Synthesis, coordination properties and biological activity of vanadium complexes with hydrazone Schiff base ligands, *Polyhedron*, 185, 114589.

[18] Abdulghani, A.J., and Abbas, N.M., 2011, Synthesis characterization and biological activity study of new Schiff and Mannich bases and some metal complexes derived from isatin and dithiooxamide, *Bioinorg. Chem. Appl.*, 2011, 706262.

[19] Maurya, M.R., Jangra, N., Avecilla, F., and Correia, I., 2018, 4,6-Diacetyl resorcinol based vanadium(V) complexes: Reactivity and catalytic applications, *Eur. J. Inorg. Chem.*, 2019 (2), 314–329.

[20] Nunes, P., Correia, I., Cavaco, I., Marques, F., Pinheiro, T., Avecilla, F., and Pessoa, J.C., 2021, Therapeutic potential of vanadium complexes with 1,10-phenanthroline ligands, *quo vadis*? Fate of complexes in cell media and cancer cells, *J. Inorg. Biochem.*, 217, 111350.

[21] Damena, T., Zeleke, D., Desalegn, T., Demissie, T.B., and Eswaramoorthy, R., 2022, Synthesis, characterization, and biological activities of novel vanadium(IV) and cobalt(II) complexes, *ACS Omega*, 7 (5), 4389–4404.

[22] Askari, B., Rudbari, H.A., Valente, A., Bruno, G., Micale, N., Shivalingegowda, N., and Krishnappagowda, L.N., 2020, Synthesis, characterization and anticancer studies of Rh(I), Rh(III), Pd(II) and Pt(II) complexes bearing a dithiooxamide ligand, *ChemistrySelect*, 5 (2), 810–817.

[23] Das, U., Kar, B., Pete, S., and Paira, P., 2021, Ru(II), Ir(III), Re(I) and Rh(III) based complexes as next generation anticancer metallopharmaceuticals, *Dalton Trans.*, 50 (32), 11259–11290.

[24] Zhong, H.J., Wang, W., Kang, T.S., Yan, H., Yang, Y., Xu, L., Wang, Y., Ma, D.L., and Leung, C.H., 2017, A rhodium(III) complex as an inhibitor of neural precursor cell expressed, developmentally down-regulated 8-activating enzyme with *in vivo* activity against inflammatory mowel disease, *J. Med. Chem.*, 60 (1), 497–503.

[25] Mishra, N.K., Choi, M., Jo, H., Oh, Y., Sharma, S., Han, S.H., Jeong, T., Han, S., Lee, S.Y., and Kim, I.S., 2015, Direct C-H alkylation and indole formation of anilines with diazo compounds under rhodium catalysis, *Chem. Commun.*, 51 (97), 17229–17232.

[26] Tan, T.T.Y., and Hahn, F.E., 2019, Synthesis of iridium(III) and rhodium(III) complexes bearing

C8-metalated theophylline ligands by directed C–H activation, *Organometallics*, 38 (9), 2250–2258.

[27] Naji, H.K., Al Hassani, R.A.M., and Balakit, A.A., 2022, Synthesis, characterization, and biological screening of Co(II), Ni(II), Cu(II), Pd(II), and Pt(IV) complexes of a novel hydrazide–hydrazone ligand derived from gallic acid, *J. Pharm. Negat. Results*, 13 (4), 1152–1159.

[28] Abdulsada, Z.S., Hassan, S.S., and Awad, S.H., 2023, Synthesis, characterization and biological activity of new oleander complexes against bacteria found in polluted water, *Indones. J. Chem.*, 23 (6), 1638–1651.

[29] Ward, H.A., Musa, T.M., and Nasif, Z.N., 2022, Synthesis and characterization of some transition metals complexes with new ligand azo imidazole derivative, *Al-Mustansiriyah J. Sci.*, 33 (2), 31–38.

[30] Al-Alzawi, S.M., Al-Jibouri, M.N., Rasheed, A.M., and Al-Bayati, S.M., 2023, Synthesis, characterization and antimicrobial activity of complexes metal ions Ni(II), Zn(II), Pd(II) and Pt(IV) with polydentate 1,2,4-triazole ligand, *Indones. J. Chem.*, 23 (1), 210–218.

[31] Kooij, B., Zhaowen, D., Varava, P., Fadaei-Tirani, F., Scopelliti, R., Piveteau, L., and Severin, K., 2022, Vanadium complexes with *N*-heterocyclic vinylidene ligands, *Chem. Commun.*, 58 (26), 4204–4207.

[32] Justim, J.R., Bohs, L.M.C., Martins, B.B., Bandeira, K.C.T., de Melo, A.P.L., Gervini, V.C., Bresolin, L., Godoi, M., and Peixoto, C.R.M., 2021, Electrochemical characterization of isatin-thiosemicarbazone derivatives, *J. Chem. Sci.*, 133 (4), 124.

[33] Reda, S.M., and Al-Hamdani, A.A.S., 2023, Mn(II), Fe(III), Co(II) and Rh(III) complexes with azo ligand: Synthesis, characterization, thermal analysis and bioactivity, *Baghdad Sci. J.*, 20 (3), 642–660.

[34] Kumari, A., 2019, Analysis of transition metal complexes of rhodium(III) containing trans–(14)–diene, *Int. J. Adv. Acad. Stud.*, 1 (1), 76–78.

[35] Al-Bayati, S., Alazawi, S., Al-Barody, S., Rasheed, A., and Alhassani, R., 2024, Synthesis of manganese(II), iron(III), and vanadium(IV) complexes with new Schiff bases and their spectroscopic and thermal studies and evaluation of their antimicrobial activity, *J. Turk. Chem. Soc., Sect. A*, 11 (1), 103–114.

[36] Yusenko, K.V., Sukhikh, A.S., Kraus, W., and Gromilov, S.A., 2020, Synthesis and crystal chemistry of octahedral rhodium(III) chloroamines, *Molecules*, 25 (4), 768.

[37] Sharma, B.P., Pandey, S.K., Marasini, B.P., Shrestha, S., and Sharma, M.L., 2021, Oxovanadium(IV) complexes with triazole based Schiff base ligands: Synthesis, characterization and antibacterial study, *J. Nepal Chem. Soc.*, 42 (1), 56–63.